

Magnetohydrodynamic Mechanism for Pedestal Formation

L. Guazzotto and R. Betti

*Department of Mechanical Engineering, University of Rochester, Rochester, New York, 14627
and Princeton Plasma Physics Laboratory, Princeton, New Jersey, 08540, USA*

(Received 4 March 2011; published 16 September 2011)

Time-dependent two-dimensional magnetohydrodynamic simulations are carried out for tokamak plasmas with edge poloidal flow. Differently from conventional equilibrium theory, a density pedestal all around the edge is obtained when the poloidal velocity exceeds the poloidal sound speed. The outboard pedestal is induced by the transonic discontinuity, the inboard one by mass redistribution. The density pedestal follows the formation of a highly sheared flow at the transonic surface. These results may be relevant to the L - H transition and pedestal formation in high performance tokamak plasmas.

DOI: 10.1103/PhysRevLett.107.125002

PACS numbers: 52.30.Cv, 52.55.Fa, 52.65.Kj

Understanding energy transport in tokamaks is critical to the development of controlled nuclear fusion. To achieve burning plasma conditions, the thermal energy must be confined for a sufficiently long time (~ 1 s) and the edge transport properties play an important role in determining the confinement time. In tokamak experiments, two distinct confinement regimes are observed, the so-called low (L) and high (H) confinement modes. In H mode [1], the confinement time can be a factor of 2 or more longer than in L mode, making H -mode operation highly desirable for future experiments and reactors. L - H transitions [2] are observed to occur spontaneously in experiments when an input heating power threshold is exceeded. H modes are characterized by steep density gradients (pedestals) near the edge and by high rotation shear across the pedestal region, with the poloidal (the short way around the torus) velocity changing by several km/s across a narrow layer. In this Letter, we identify a possible mechanism that can play an important role in the L - H transition. This mechanism is a purely magnetohydrodynamic effect that develops when the edge plasma poloidal flow exceeds the poloidal sound speed C_{sp} . Since the edge poloidal sound speed is typically in the range of a few tens km/s, this mechanism requires minimum poloidal velocities of that same order. Using time-dependent two-dimensional compressible MHD simulations, we show that a pedestal in density and a strongly sheared velocity profile develop in poloidally rotating plasmas. We refer to this mechanism as the MHD pedestal to emphasize the MHD character of the physics, and conjecture that the sheared velocity profile causes an edge transport barrier. Equilibrium calculations [3,4] also predict a density pedestal for transonic poloidal flows. However, contrary to the observations, the standard pedestal height from equilibrium theory is highly nonuniform [$\sim \cos(\theta/2)$, where θ is the poloidal angle] and vanishes on the high-field (inner) side (see Fig. 11 of Ref. [4]). A new effect (poloidal redistribution of mass) is identified by 2D simulations described in this Letter, which produces a pedestal of finite height at every angular

location, consistent with experiments. In order to distinguish between the characteristics of the pedestal in the inboard and in the outboard part of the plasma, we refer to the first one as the inner pedestal and to the latter as the transonic pedestal (to emphasize its connection with transonic poloidal flow). This Letter does not address important aspects of the L - H transition and/or pedestal formation, such as the origin of the edge poloidal flow, the pedestal stability [5], and evolution over the transport time scale. The only claim of this Letter is that a rotating plasma develops an edge density pedestal and a velocity shear layer when the poloidal velocity V_p exceeds the poloidal sound speed $C_{sp} = C_s B_p / B$ (B_p and B are the poloidal and total B field, respectively). The simulations shown here are limited to short time scale evolutions of the order of a few poloidal revolutions, and their relevance is likely restricted to the early onset of the L - H transition and pedestal formation.

There are some features of the MHD pedestal formation that nicely fit the experimental observations of the L - H transition. For instance, according to this theory, plasmas with a lower edge poloidal sound speed require lower edge poloidal flows for the MHD pedestal formation. This agrees with the observations that the power threshold for the L - H transition decreases in the presence of an X point close to the plasma. Since the poloidal sound speed vanishes at the X point, a lower poloidal rotation is required to exceed C_{sp} at the plasma edge. Furthermore, it was observed that the L - H power threshold is even lower in “true” double-null configurations [6] where C_{sp} vanishes on two points of the outer surface. A double-null plasma minimizes C_{sp} and would require a lower edge V_p for the development of the MHD pedestal. A number of experiments [7] reported that the L - H power threshold decreases with the ion mass. Since C_{sp} decreases with the ion mass, we conjecture that the MHD pedestal formation is also facilitated in plasmas with higher m_i .

The physics basis of the MHD pedestal theory resides on the development of the so-called transonic discontinuity

identified in the analytic theory of Refs. [3,4]. In transonic equilibria, the poloidal velocity is slower than the poloidal sound speed (subsonic) in the plasma core and faster near the edge (supersonic). In Ref. [3], it is shown with a simplified analytic model, that toroidal geometry causes the transition between the two regions to occur through a radial tangential discontinuity. Because of the frozen-in law, the plasma must flow between adjacent magnetic surfaces; due to the toroidal geometry, the cross section for poloidal flow is maximum on the outboard side of the plasma and minimum on the inboard. Basic gas-dynamic considerations indicate that a flow stream that is subsonic (supersonic) on the inner midplane will decelerate (accelerate) as it moves toward the outboard part of the plasma. Thus two adjacent streams, one just subsonic on the inner midplane and one just supersonic, will see the difference in their Mach numbers increase as they move toward the outer midplane generating radially discontinuous profiles. It is stressed that the equilibrium discontinuity is not a shock but a tangential discontinuity; i.e., there is no flow across the discontinuity. Figure 1 shows a sketch of the expected discontinuity in velocity.

In the remainder of this Letter, it is shown how a static equilibrium naturally evolves to form discontinuous profiles when a (continuous) momentum source is applied to the plasma. The origin of the momentum source is not addressed here. The only assumption is that the source is a smooth function of space and strong enough to accelerate the edge plasma to velocities above the local poloidal sound speed.

The basic description of the plasma is given by the time-dependent MHD model. The computational domain includes the main plasma and a “halo” plasma region, with cold, low-density plasma, and open field lines. Ideal MHD is sufficient to capture the essential physics in the core region, while the halo region is better represented as a resistive plasma. Therefore, the resistive-MHD set of equations is used:

$$\partial_t \rho + \nabla \cdot (\rho \underline{V}) = 0, \quad (1)$$

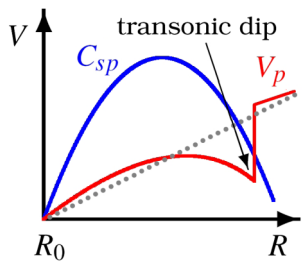


FIG. 1 (color online). Sketch of poloidal velocity (red) and poloidal sound speed (blue). The profile represented with a dotted line is not allowed at steady state by MHD force balance. The discontinuous solid line is the only possible transonic solution.

$$\partial_t \rho \underline{V} + \nabla \cdot (\rho \underline{V} \underline{V} - \underline{B} \underline{B} + P \underline{I} + \underline{\Pi}) = \underline{S}_{\text{mom}}, \quad (2)$$

$$\partial_t \underline{B} = \nabla \times (\underline{V} \times \underline{B} - \eta \underline{J}), \quad (3)$$

$$\partial_t \mathcal{E} + \nabla \cdot [(\mathcal{E} + P) \underline{V} - \underline{B}(\underline{V} \cdot \underline{B}) + \eta \underline{J} \times \underline{B}] = \underline{V} \cdot \underline{S}_{\text{mom}}, \quad (4)$$

where \underline{B} is the magnetic field, \underline{V} the plasma velocity, ρ the density, \underline{J} the current, $P \equiv p + B^2/2$ the total pressure, $\mathcal{E} = \frac{p}{\gamma-1} + \rho \frac{V^2}{2} + \frac{B^2}{2}$ the total energy, γ the adiabatic index, η the resistivity, and the pressure tensor $\underline{\Pi}$ represents numerical viscosity. Resistivity is defined using Spitzer’s formula, $\eta \sim T^{-3/2}$, and the temperature $T \sim p/\rho$ is self-consistently evolved using Eqs. (1)–(4). Qualitatively, results do not depend on the value of γ . Here we use $T_e = T_i$ and the typical isothermal condition $\gamma \approx 1$ valid for large parallel heat conduction. The source term of poloidal momentum $\underline{S}_{\text{mom}}$ is added to Eqs. (2) and (4) in order to drive the flow. The strength of the source is a smooth function of position (e.g., of distance from the edge) or of the initial poloidal flux ψ , and optionally of the poloidal angle. The system of time-dependent equations (1)–(4) is solved with the code SIM2D. SIM2D is written in conservative form with a finite-difference numerical implementation using a combination of a predictor-corrector and an alternate-direction implicit methods.

Based on the physical argument summarized earlier and in Ref. [3], the following qualitative behavior is expected for a transient with transonic poloidal flow. Once the flow becomes supersonic (with respect to the poloidal sound speed C_{sp}), a shock will form in the outboard section of the plasma. Shock formation is a transient phenomenon consequence of the compressible MHD model. The shock quickly moves in the poloidal direction, reaches the inner midplane, and disappears. The flow transports mass from the outboard to the inboard part of the plasma: The mass accumulation on the inboard side of the plasma also generates a steep density profile, thus providing a final state with a pedestal at every poloidal location. No shocks persist in the final plasma state, only the tangential discontinuity or MHD pedestal. At this point the plasma is divided in two regions: a supersonic outer region and a subsonic inner region (Fig. 1). The transition between the two regions occurs with a finite discontinuity (in Mach number, density, velocity, pressure) that we denote as the “MHD pedestal.” Mach number and velocity are radially continuous in the inboard part of the plasma. Nevertheless, a density pedestal also develops at the inner midplane, due to the mass transported in the poloidal direction. In tokamaks, the long particle mean free path may prevent the shock formation. However, since the final state is shockless, the quick shock transient introduced by compressible MHD (and probably unphysical in real tokamaks) should not alter the validity of the results with respect to the final state. This is also true for

the formation of the inner pedestal. Since the equilibrium MHD density for supersonic poloidal flows is much smaller than the corresponding subsonic density, at steady state part of the mass initially in the outboard region must necessarily have moved to the inboard region, regardless of the presence of a shock.

We now show some numerical results, proving the formation of the MHD pedestal with time-dependent simulations starting from an L -mode plasma equilibrium. A DIII-D lower single null model equilibrium is used as the initial condition for our simulations with the only purpose to capture some reasonable experimental parameters and provide the grounds for a proof-of-principle simulation. The main equilibrium parameters are $\beta_t = 1.1\%$ (β_t is the ratio between average pressure and vacuum magnetic pressure), plasma current $I_p = 721$ kA, and vacuum toroidal field of $B_V = 1.26$ T. We assume an edge temperature of $T_E \sim 30$ eV (T_E determines the edge sound speed, $C_{sp} \lesssim 20$ km/s at the edge) and a peak temperature of $T_C = 3$ keV. Plasma temperature and density are initially constant in the halo region and equal to their edge values. A three-dimensional sketch of the initial equilibrium is shown later in Fig. 4. In this case, the momentum source is assigned as $S_{\text{mom}} \sim \rho \psi^2 \cos(\theta/2)$ (θ is the poloidal angle). The poloidal angle dependence is used to qualitatively reproduce the shape of poloidal flow generation by nonuniform phenomena, like, for instance, turbulence driven by unfavorable curvature or radial electric fields caused by particle losses. The radial dependence describes a volumetric source of momentum that is peaked at the plasma edge. The dependence on ρ guarantees that the velocity source is smooth, so that the velocity discontinuity after the pedestal formation cannot be ascribed to the source shape since the density cancels when the acceleration and the source are balanced, $\partial_t V_p \sim S_{\text{mom}}/\rho \sim \psi^2$. A more realistic shape of S_{mom} requires considerations related to the origin and the transport of momentum that are outside the scope of this Letter. The intent here is to show that a smooth source of momentum causes a MHD pedestal when the plasma is accelerated above the poloidal sound speed. There is no physical dissipation in the simulations (only numerical viscosity), so that a weak momentum source is sufficient to create the MHD pedestal. In future work, neoclassical poloidal viscosity will be included in the model and a realistic power threshold for the pedestal generation will be estimated. This will require a transonic poloidal viscosity model valid for supersonic speeds [8].

In presenting the simulation results, we normalized the time to τ_p , an average revolution time considering an edge velocity of ~ 40 km/s, consistent with experiments. The source strength is measured through the dimensionless parameter $\hat{S} = (L_p S_{\text{mom}} B^2 / \gamma B_p^2 \rho)_{M=1}$ representing the ratio $\tau_{sp} / \tau_{\text{source}}$ between the time of a sound wave poloidal revolution τ_{sp} and the time required for the source of momentum to spin up the plasma at the poloidal speed of

sound ($L_p \sim 2\pi r_{M=1}$ is the poloidal revolution length). In the simulations, we use $\hat{S} \approx 12$ to quickly spin up the plasma to poloidal sonic velocities thus reducing the simulation time. The poloidal flow becomes supersonic after a time $\approx 0.1\tau_p$ and a shock forms in the outboard region, which then travels in the poloidal direction. The duration of the transient depends on the size of the source. A lower intensity source leads to a longer transient but will not affect the final state. In the run described here, the shock reaches the inboard section of the plasma in $\approx 0.8\tau_p$; after this time, a discontinuity is formed in density, velocity, and Mach number profiles. The shape of the density profile at time $t = 2.5\tau_p$ is shown in Fig. 2 (gray line) and compared to the initial density profile. The sharpening of the density gradient in both the inboard and outboard regions is clearly visible. The difference between the two pedestals is recognized from their position with respect to the supersonic region (shaded in the figure). The inner pedestal is entirely in the supersonic region (i.e., it is not due to the transonic jump in Mach number), while the transonic pedestal extends between the subsonic and the supersonic regions. The shape of the poloidal velocity and Mach number profiles is shown in Fig. 3. The sharp gradient in the outboard region for both profiles (due to the transonic discontinuity) is in clear contrast with both the smooth profiles in the inboard region and the smooth profile of the velocity source. The radial electric field E_r (not shown) has a shape similar to the poloidal velocity shape and a peak value of ~ 30 – 40 [kV/m] after the MHD pedestal formation. The velocity profile shows the presence of a minimum (“transonic dip”) before the MHD pedestal region, similar to experimental profiles [9,10]. The maximum velocity in Fig. 3 is ≈ 40 km/s, of the same order of the measured main-ion poloidal velocity in DIII-D [10]. Since there is no

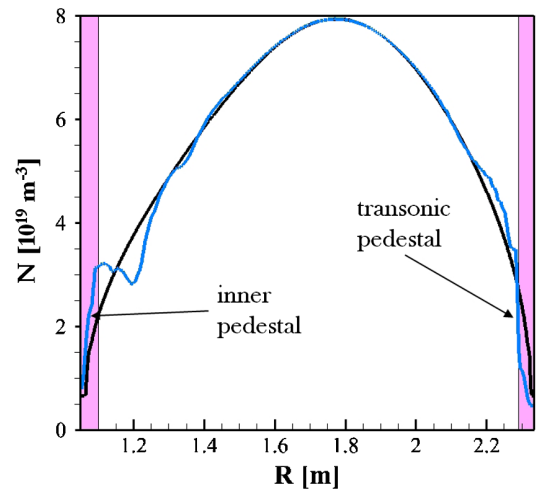


FIG. 2 (color online). Density plot along the midplane at time $t = 2.5\tau_p$. The shaded area corresponds to the region with supersonic flow.

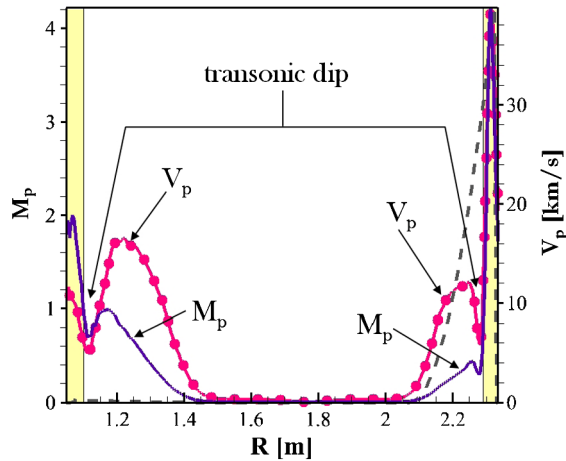


FIG. 3 (color online). Poloidal velocity and Mach number along the midplane at time $t = 2.5\tau_p$. The dashed line represents the velocity source (in arb. units). The shaded area corresponds to the region with supersonic flow.

physical viscosity in the simulations, the source must be reduced once the shock transient is over. The density pedestal structure and the velocity shear layer shown in Figs. 2 and 3 do not appreciably change after the initial transient. Additional insight on the characteristics of the transonic pedestal is gained by considering a three-dimensional representation of the plasma density, as shown in Fig. 4. Figure 4(a) shows the initial density profile (both in color map and elevation), while Fig. 4(b) shows the density for the quasisteady state of the SIM2D simulation, highlighting the presence of the inner pedestal in the inboard and of the transonic pedestal in the outboard region. The black line in Fig. 4(b) corresponds to the level $M_p = 1$: the $M_p = 1$ line runs in the middle of the transonic pedestal (which is a transonic discontinuity) but on one side of the inner pedestal (which is due to the poloidal transport of mass). Because of the lack of physical dissipation (which prevents simulations from reaching a true steady state) and the effect poloidal redistribution of mass, SIM2D quasisteady states are similar, but not identical, to the standard transonic equilibria calculated with FLOW [11].

No details were given about the origin of the momentum source. This is intentional, since the described mechanism for the MHD pedestal formation does not depend on any specific source: if the plasma is made to spin with transonic poloidal velocity, a MHD pedestal will form, regardless of the origin of the spin-up. It is important to point out that poloidal velocities of the order of the poloidal sound speed are larger than neoclassical values [12]. However, such velocities are observed in experiments [13,14], and several mechanisms have been proposed for poloidal spin-up. An intuitive mechanism is due to nonambipolar losses at the edge [15], producing a radial electric field at the plasma edge (due, e.g., to fast-ion losses) that drives a poloidal

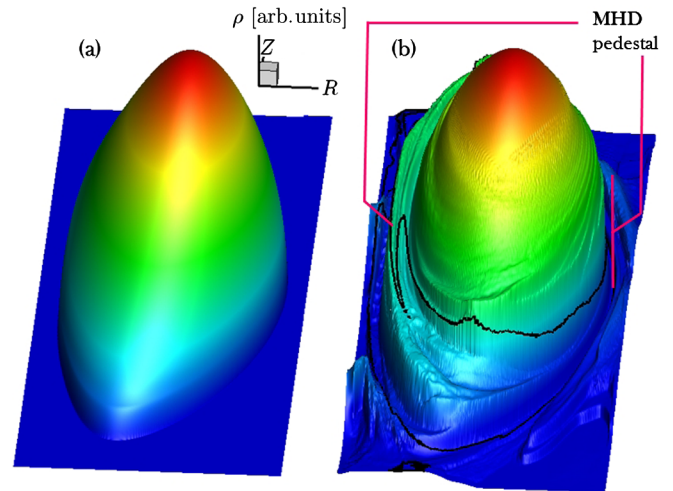


FIG. 4 (color online). Three-dimensional density plot at time $t = 0$ (a) and $t = 2.5\tau_p$ (b).

flow. Other known mechanisms for plasma spin-up include turbulent spin-up [16,17] and resistive spin-up [18].

A MHD pedestal formation mechanism was described and verified with numerical simulations. Several experimental clues are found that seem to indicate that MHD transonic discontinuities may play a role in the L - H transition. A more definite experimental confirmation can be provided by direct measurements of the main ion poloidal flow at the plasma edge and the identification of the transonic dip (Fig. 3).

This work was supported by DOE under Grant No. DE-FG02-93ER54215.

-
- [1] F. Wagner *et al.*, *Phys. Rev. Lett.* **49**, 1408 (1982).
 - [2] K. H. Burrell *et al.*, *Plasma Phys. Controlled Fusion* **34**, 1859 (1992); J. W. Connor and H. R. Wilson, *Plasma Phys. Controlled Fusion* **42**, R1 (2000).
 - [3] R. Betti and J. P. Freidberg, *Phys. Plasmas* **7**, 2439 (2000).
 - [4] L. Guazzotto, R. Betti, J. Manickam, and S. Kaye, *Phys. Plasmas* **11**, 604 (2004).
 - [5] P. B. Snyder *et al.*, *Phys. Plasmas* **9**, 2037 (2002); P. N. Guzdar, S. M. Mahajan, and Z. Yoshida, *Phys. Plasmas* **12**, 032502 (2005).
 - [6] H. Meyer *et al.*, *Nucl. Fusion* **46**, 64 (2006).
 - [7] P. Gohil, T. C. Jernigan, J. T. Scoville, and E. J. Strait, *Nucl. Fusion* **49**, 115004 (2009).
 - [8] K. C. Shaing and P. J. Christenson, *Phys. Fluids B* **5**, 666 (1993); A. B. Hassam, *Nucl. Fusion* **36**, 707 (1996).
 - [9] R. M. McDermott *et al.*, *Phys. Plasmas* **16**, 056103 (2009), see Fig. 9 (figure refers to perpendicular velocity).
 - [10] J. Kim *et al.*, *Phys. Rev. Lett.* **72**, 2199 (1994).
 - [11] L. Guazzotto and R. Betti, *Phys. Plasmas* (to be published).
 - [12] M. N. Rosenbluth and F. L. Hinton, *Phys. Rev. Lett.* **80**, 724 (1998).

- [13] K.D. Marr *et al.*, *Plasma Phys. Controlled Fusion* **52**, 055010 (2010) (measurements refer to flow of impurities).
- [14] W.M. Stacey and R.J. Groebner, *Phys. Plasmas* **15**, 012503 (2008).
- [15] K.C. Shaing and E.C. Crume, *Phys. Rev. Lett.* **63**, 2369 (1989).
- [16] W.J.T. Bos, S. Neffaa, and K. Schneider, *Phys. Rev. Lett.* **101**, 235003 (2008).
- [17] H.J.H. Clercx, S.R. Maassen, and G.J.F. van Heijst, *Phys. Rev. Lett.* **80**, 5129 (1998).
- [18] T.E. Stringer, *Phys. Rev. Lett.* **22**, 770 (1969).